SUPPLEMENT

The *Rickettsia* surface cell antigen 4 applies mimicry to bind to and activate vinculin

HaJeung Park[‡], Jun Hyuck Lee[‡1], Edith Gouin[§¶‖], Pascale Cossart[§¶‖], and Tina Izard[‡2]

From the [‡]Cell Adhesion Laboratory, Department of Cancer Biology, The Scripps Research Institute, Jupiter, Florida 33458 and [§]Unité des Interactions Bactéries-Cellules, Institut Pasteur, France F-75015, [¶]INSERM, U604, Paris F-75015, and [‖]INRA, USC2020, Paris F-75015

[1]Present address: Division of Polar Life Sciences, Korea Polar Research Institute, Incheon 406-840, South Korea
[2]To whom correspondence should be addressed. Tel: 1-561-228-3220; Fax; 1-561-228-3068; E-mail: mkernick@scripps.edu

Supplementary Methods

Analytical size exclusion chromatography - The protein concentrations were calculated from the protein absorbance at 280 nm and their molar extinction coefficient. 100 units of bovine thrombin (Sigma-Aldrich) were added to 40 mg of each protein and incubated overnight at 4 ºC. SDS-PAGE analysis showed that the efficiency of the digestions were nearly 100%. The proteins were then run on a size exclusion chromatography column for further purification. The stoichiometry of sca4 and Vh1 was determined by analytical size exclusion chromatography. Briefly, sca4 residues 21-1008 or 411-1008 were mixed with Vh1 in molar ratios of 4:1, 2:1, and 1:1 in running buffer containing 150 mM NaCl, 2 mM DTT, and 10 mM Tris-HCl (pH 7.5). Sca4 and Vh1 (also in the running buffer) were incubated at room temperature for 20 min prior to analysis on an Äkta FPLC system (GE Healthcare) equipped with a Superdex 200 10 X 300 GL (GE Healthcare) sizing chromatography column. A flow rate of 0.5 ml/min was used and the peak fractions were collected and analyzed by SDS-PAGE.

Supplementary Figure Legends

Supplementary Figure S1. The cell surface antigen sca4 of *Rickettsia rickettsii* harbors two vinculin binding sites (VBSs).
Binding stoichiometry of sca4:Vh1 complexes were measured by size-exclusion chromatography. Vh1 and sca4 proteins harboring both sca4-VBSs [(*A*) residues 21-1008 and (*B*) residues 411-1008] were mixed in 4:1, 2:1, and 1:1 molar ratios (first, second, and third chromatograms, respectively) and loaded on a Superdex 200 10 x 300 GL gel filtration sizing chromatography column. The last two chromatograms correspond to sca4 and Vh1 proteins loaded on their own, respectively, as indicated.

The orange dotted line corresponds to the elution position of Vh1 alone (of M_r of 29 kDa at 15.5 ml elution); green, sca4 alone [(*A*) 114 kDa, 10.2 ml, (*B*) 69 kDa, 11.8 ml]; blue, equimolar Vh1:sca4 complex formation [(*A*) 143 kDa, 9.8 ml, (*B*) 98 kDa, 11.2 ml]; and red, two Vh1 molecules binding per sca4 molecule [(*A*) 172 kDa, 9.6 ml, (*B*) 127 kDa, 10.5 ml]. At four-fold Vh1 molar excess (top chromatograms), sca4 is not saturated by Vh1 and unbound Vh1 elutes from the column while at two-fold Vh1 molar excess (second sets of chromatograms), sca4 is saturated with Vh1 and no remaining Vh1 is eluted. Finally, at equimolar ratio (third pairs of chromatograms), Vh1 remains depleted while the Vh1:sca4 complex peak is shifted compared to the earlier Vh1:sca4:Vh1 complex peak.

Supplementary Figure S2. Identification of fractions.
SDS-PAGE (8-25% gradient) analysis of fractions from the top two chromatograms shown in Supplementary Figure S1 identifying the first and second peak as Vh1:sca4 complex and Vh1 alone, respectively.
Top gel [Vh1:sca4-21-1008 complex peak; first peak of top chromatogram of panel (*A*) in Supplementary Figure S1]: 8.5 ml (lane 1), 9 ml (lane 2), 9.5 ml (lane 3), 10 ml (lane 4), 10.5 ml (lane 5), 11 ml (lane 6); *middle gel* [Vh1 peak; second peak of top chromatogram of panel (*A*) in Supplementary Figure S1]*:* 14 ml (lane 1), 14.5 ml (lane 2), 15 ml (lane 3), 15.5 ml (lane 4), 16 ml (lane 5); and *bottom gel* [Vh1:sca4-411-1008 peak; first peak of top chromatogram of panel (*B*) in Supplementary Figure S1]*:* 9.5 ml (lane 1), 10 ml (lane 2), 10.5 ml (lane 3), 11 ml (lane 4), 14.5 ml (lane 5), 15 ml (lane 6), and 15.5 ml (lane 7).

Supplementary Figure S3. Stereo view of Vh1:VBS superposition as shown in Figure 4A.
Superposition of all known talin-VBSs and IpaA-VBSs in their Vh1-bound states (white) onto our 2 Å Vh1:sca4-VBS-N (green) and 2.8 Å Vh1:sca4-VBS-C (magenta) crystal structures. Vh1 is shown as a Cα trace and the VBSs as a cartoon. Vh1 α-helices α4-α7 are labeled. All VBSs (talin-VBS1, residues 608-627; talin-VBS11, residues 822-841; talin-VBS2, residues 855-874; talin-VBS33, residues 1525-1544; talin-VBS36, residues 1633-1652; talinVBS58, residues 2345-2364; IpaA-VBS1; and IpaA-VBS2) were aligned to talin-VBS3 (residues 1949-1968) with *r.m.s.d.* ranging from 0.5 Å to 1.1 Å. Sca4-VBS-C induces a significant movement of the *C*-terminal Vh1 four-helix bundle subdomain, which is unique versus all other Vh1:VBS structures.

Supplementary Figure S4. Stereo view of zoomed in views of Vh1:sca4-VBS-N superimposed onto Vh1:sca4-VBS-C as shown in Figures 4B and 4C.
A. Zoomed in stereo view of the superposition of sca4-VBS-N (green) which is representative of all Vh1:VBS structures onto the sca4-VBS-C (magenta) in their Vh1-bound states. Unlike other VBSs, sca4-VBS-C has two acidic residues on its *N*-terminus

(Asp-812 is shown in sticks and is labeled), which might stabilize the sca4-VBS-C α-helix by neutralizing its dipole. The large movement of the *C*-terminal Vh1 subdomain is indicated by the movement of Lys-173 and the arrow.

B. Zoomed in stereo view showing the kink at sca4 Pro-827 (shown in black sticks, labeled) in sca4-VBS-C (magenta) compared to the sca4-VBS-N (green); the latter is representative of all other Vh1:VBS structures. Residues amino-terminal to Pro-827 moved while the carboxy-terminal ends superimpose well. This movement causes Vh1 α-helix α1 to shift down (in this view) and towards the *C*-terminal Vh1 subdomain as indicated by the arrow.

Supplementary Figure S5. Sca4-VBS-N binding to the vinculin head domain Vh1.
Stereo view of the final $2F_o$-F_c electron density map calculated using autoBUSTER for sca4-VBS-N (yellow) bound to Vh1 (green). The contour level of the electron density map is 0.7σ and the resolution is 2 Å. Electron density was not visible for the side chain of Gln-211, which was therefore not modeled.

Supplementary Figure S6. Sca4-VBS-C binding to the vinculin head domain Vh1.
Stereo view of the final $2F_o$-F_c electron density map calculated using autoBUSTER for sca4-VBS-C (yellow) bound to Vh1 (green). The contour level of the electron density map is 0.7σ and the resolution is 2.8 Å. Electron density was not visible for residues 30-33 and for the side chains of Lys-35, Ile-37, and Lys-228, which were therefore not modeled.

Supplementary Figure S7. Comparison of vinculin interactions with each sca4-VBS.
Vinculin residues are in black font and sca4-VBS residues are in blue font. Vinculin residues on the left of sca4 residues engage in polar interactions, while vinculin residues on the right of sca4 engage in hydrophobic interactions. Sca4-VBS-N (*A*) and sca4-VBS-C (*B*) residues on the same line are structurally equivalent (*e.g.*, sca4-VBS-N residue Leu-413 is structurally equivalent to sca4-VBS-C residue Ile-814).

Supplementary Figure S8. The vinculin Vh1 domain bound to sca4-VBS-C differs significantly from Vh1 bound to sca4-VBS-N or as seen in the full-length vinculin structure.
Superposition of the structurally similar region of the *N*-terminal four-helix bundle subdomain of Vh1 (residues 50-125) of the sca4-VBS-C bound (magenta) or unbound full-length vinculin (Vt and Vh1, grey; Vh2, Vh3, Vt2 domains, cyan) conformation onto the sca4-VBS-N bound (green) conformation results in *r.m.s.d.* of 0.6 Å or 1.3 Å for 489 or 525 atoms, respectively. The distinct positions of the sca4-VBS *C*-termini are

indicated by the last sca4-VBS-N and sca4-VBS-C residues being labeled (434 and 834), respectively which causes Vh1 α-helix α1 (labeled) to move upon sca4-VBS binding and to distort the Vh1-Vt interface. However, the *N*-termini (not labeled) of the sca4-VBSs adopt similar conformations. Similar to the other thirteen Vh1:VBS structures, the movements of the Vh1 *C*-terminal four-helix bundle subdomain are much more subtle in the sca4-VBS-N bound Vh1 structure, while this domain moves about 25 Å as shown by the double arrow pointing to the carboxy-terminus of Vh1 α-helix α6. Residues 3 in the Vh1:sca4-VBS-N and 1062 in the full-length human vinculin structure are labeled. The disordered region in full-length vinculin (residues 844-876) is indicated by dots. Vinculin α-helices are drawn as cylinders while sca4 is shown as a Cα trace. Vh1 α-helices are labeled α1 through α7 while Vt α-helices are labeled as H1 through H5.

Supplementary Figure S9. Further movements of Vh1 α-helix α1 in the sca4-VBS-C bound structure.
View of the superposition shown in Supplementary Figure S8 looking down the Vh1 α-helix α1. As first seen in the Vh1:talin-VBS3 structure, the binding of the sca4-VBSs distorts the Vh1-Vt interface, indicated by the labeling of the various α1 positions. The distinct positions of the sca4-VBS *C*-termini are indicated by the last sca4-VBS-N (green) and sca4-VBS-C (magenta) residues that are labeled (434 and 834, respectively), which causes the Vh1 α-helix α1 (labeled) to move upon sca4-VBS binding, distorting the Vh1-Vt interface. Note that α1 in the sca4-VBS-C bound structure moves much deeper into the core of full-length vinculin. Vh1:sca4-VBS-N is shown in green, Vh1:sca4-VBS-C in magenta, and full-length vinculin in grey (Vt and Vh1 domains) or cyan (Vh2, Vh3, Vt2 domains). Vinculin α-helices are drawn as cylinders while sca4 is shown as a Cα trace. Vh1 α-helices are labeled α1 through α7 while Vt α-helices are labeled as H1 through H5. The *C*-terminus (residue 1062) and the proline-rich regions (residues 843 and 877) in the full-length vinculin structure are labeled.

Supplementary Table. Primers used to generate the constructs in this study.

(*A)* Bacterial expression vector construction

Primer name	DNA sequence
5' NdeI 21	CGATAACATATGAATAAGGAATATACAGAA
5' NdeI 411	CGATAACATATGCCAAATCTTCTTAATGCA
5' NdeI 412	CGATAACATATGAATCTTCTTAATGCAGCT
5' NheI 412	GTACATCGCTAGCAATCTTCTTAATGCAGCTACG
5' NdeI 774	CGATAACATATGAAAGAGGCACTTAAAAAAGCT
5' NheI 812	GTACATCGCTAGCGATGATATATATAACAAAGCT
3' EcoRI 360	CGATAAGAATTCTCATTGTCCTTGTCCTATTAT
3' EcoRI 434	CGATAAGAATTCTCAACCTGCATTTACATAATT
3' EcoRI 585	CGATAAGAATTCTCAGCTTAATTCAGAGACATT
3' EcoRI 835	GTATCGGAATTCTTAAGATTTTTCTAATGCTTCTATAAC
3' EcoRI 1008	CGATAAGAATTCTCAATTTTCCGACTGAATGAT

(*B)* Mammalian expression vector construction

Primer name	DNA sequence
5' EcoRI 20	GATACGAATTCGCCACCATGGCAAATAAGGAATATACAGAAG
5' EcoRI 406	GATACGAATTCGCCACCATGTCGCAACACGTGAATCCAAATC
5' EcoRI 772	TCGAATTCTGCATCTGAGAAAGAGGCACTT
3' EcoRI 360	GATGCAGAATTCTTTGTCCTTGTCCTATTATAATATCTTC
3' EcoRI 585	GATGCAGAATTCTTAATTCAGAGACATTAACC
3' BamHI 1008	CGTAGGATCCTCAATTTTCCGACTGAATGAT
3' EcoRI 1024	GATGCAGAATTCTGCGTTGTGGAGGGGAAGACTCTC

Supplementary Figure S1

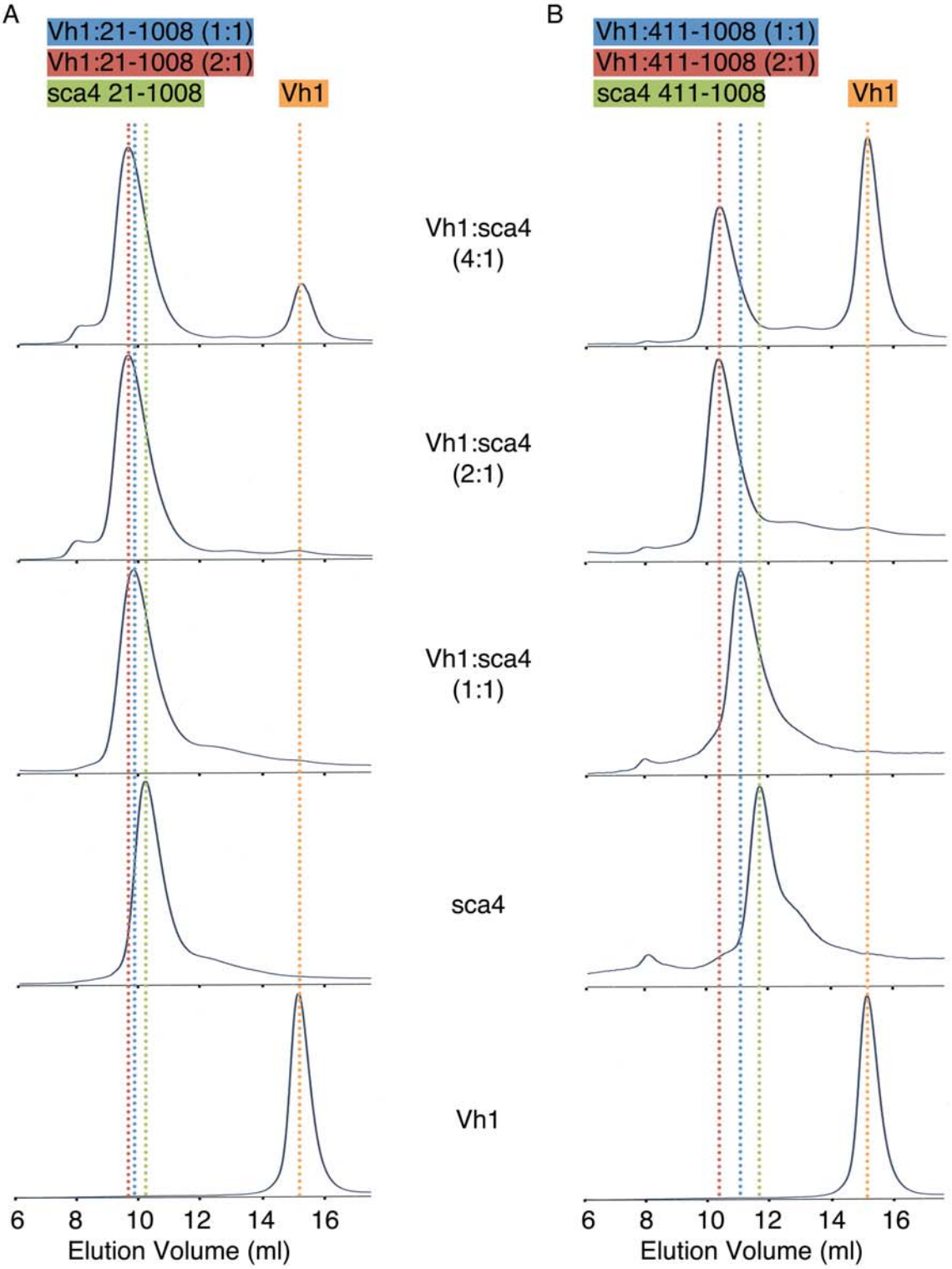

Supplementary Figure S2

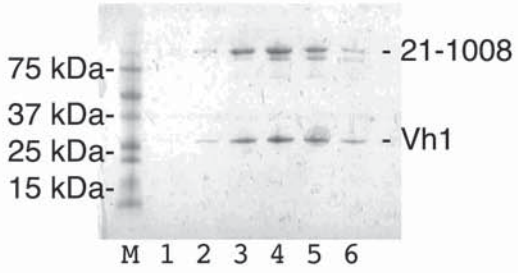

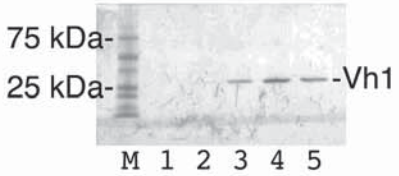

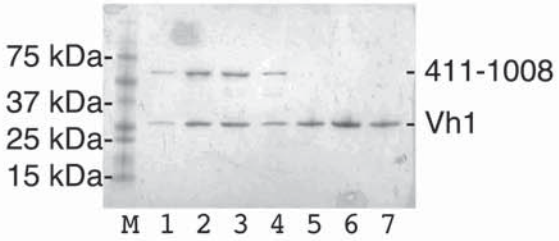

Supplementary Figure S3

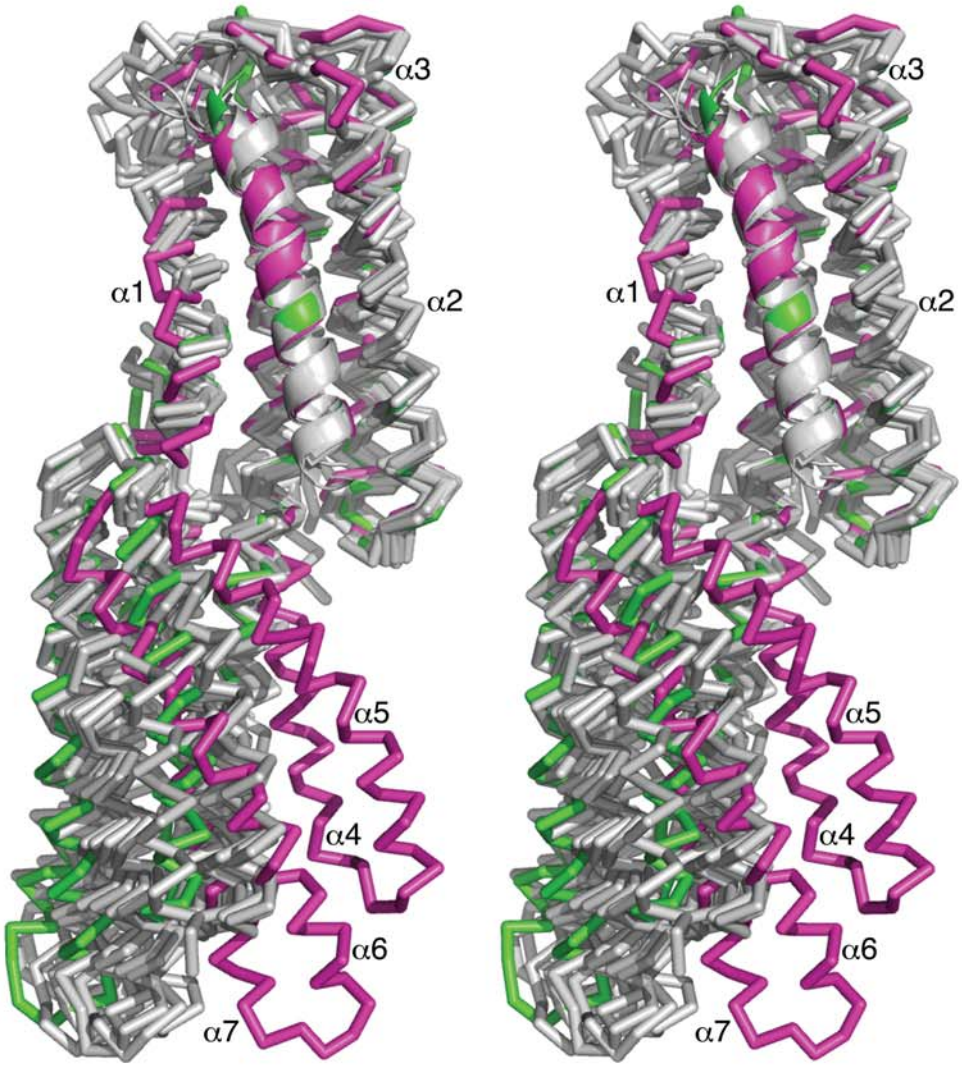

Supplementary Figure S4

A

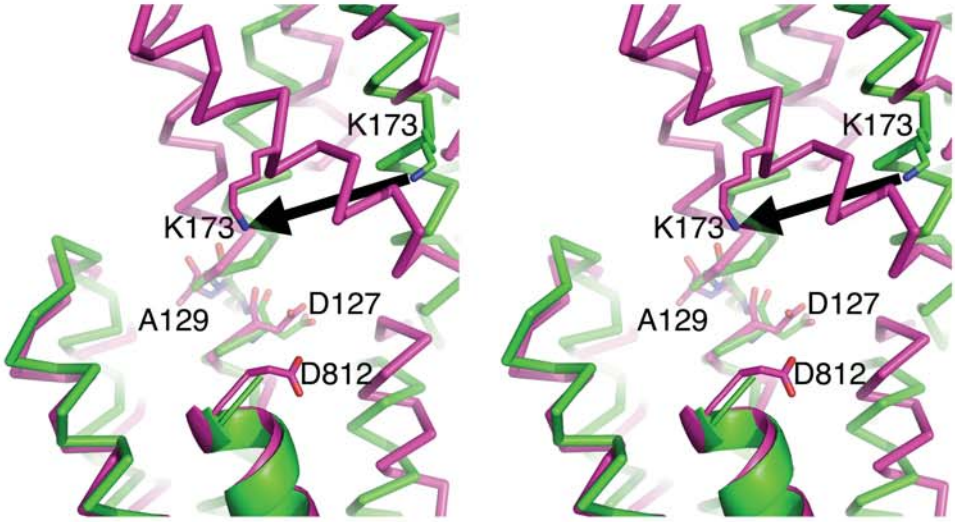

B

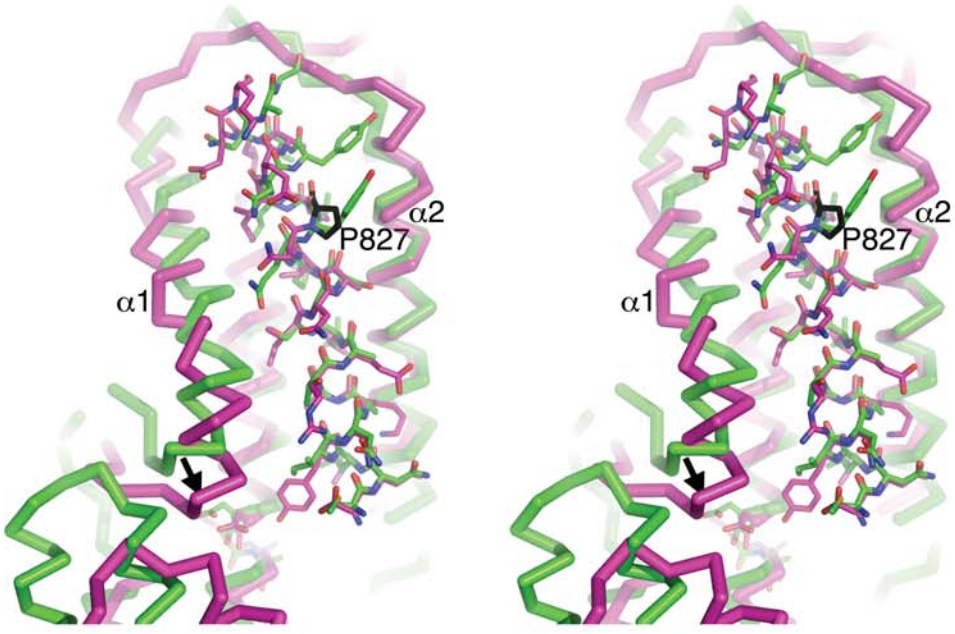

Supplementary Figure S5

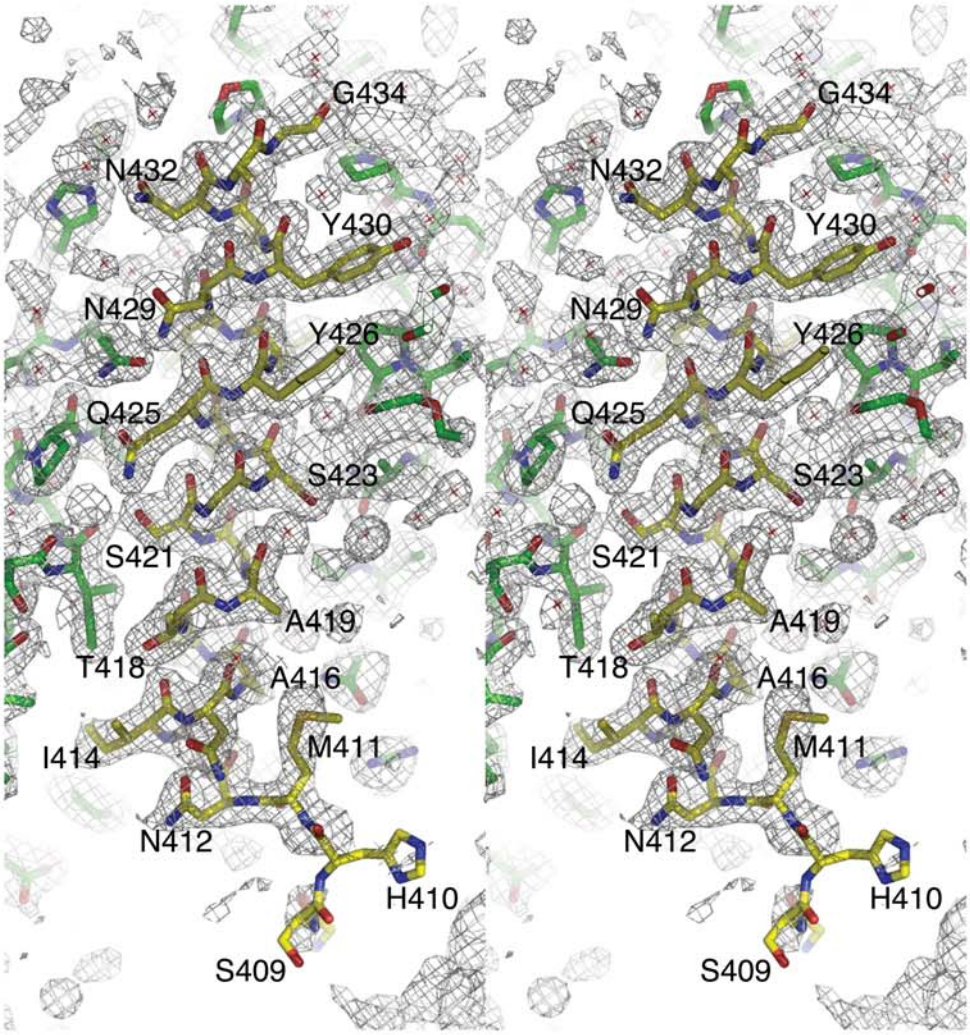

Supplementary Figure S6

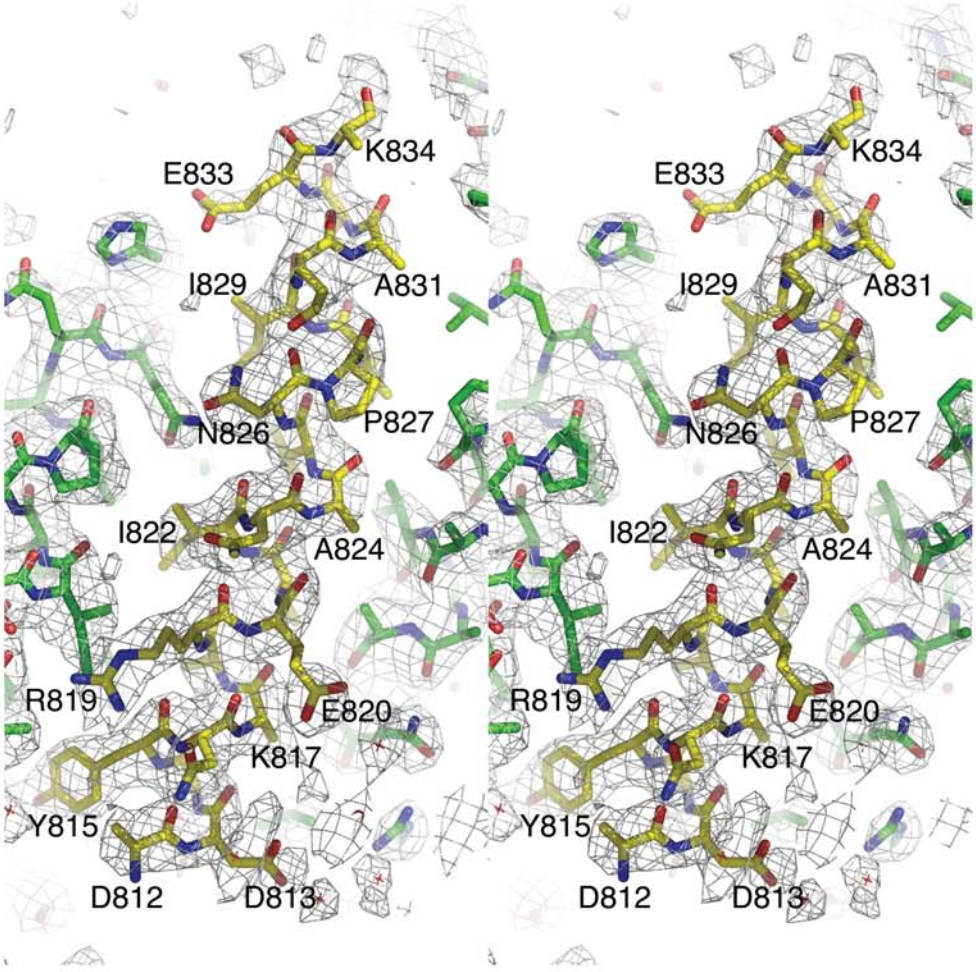

Supplementary Figure S7

A

polar Vh1	sca4-VBS-N	hydrophobic interactions Vh1
	N412	V57
	L413	L54, V57, G58, M74, F126
	L414	L123, F126
	N415	
	A416	N53, L54
	A417	I12, L123
	T418	
	A419	
	L420	V47, A50, V51, L54, I115, T119
I12	S421	I12
	G422	
	S423	V47
	M424	V47, L88, S112, I115
Q19	Q425	P15
	Y426	P43
	L427	P43, V44
	L428	Q19, I20, S112
Q19	N429	Q19
	Y430	P38, L40, P43
	V431	L23, L40, L108
H22	N432	H22
	A433	P38

B

polar Vh1	sca4-VBS-C	hydrophobic interactions Vh1
	D813	
	I814	V57
D127	Y815	T8, I9, I12, L123, F126
	N816	
	K817	L54
	A818	L54, L123
	R819	I12
	E820	
	V821	A50, L54, I115, T119
Q19	I822	I12, V16, Q19
	N823	
	A824	V47
	V825	V47, I115
Q19	N826	
	P827	
	V828	
	I829	Q19, L23
	E830	
	A831	L40
	L832	M26, L108, I109
H22	E833	H22

Supplementary Figure S8

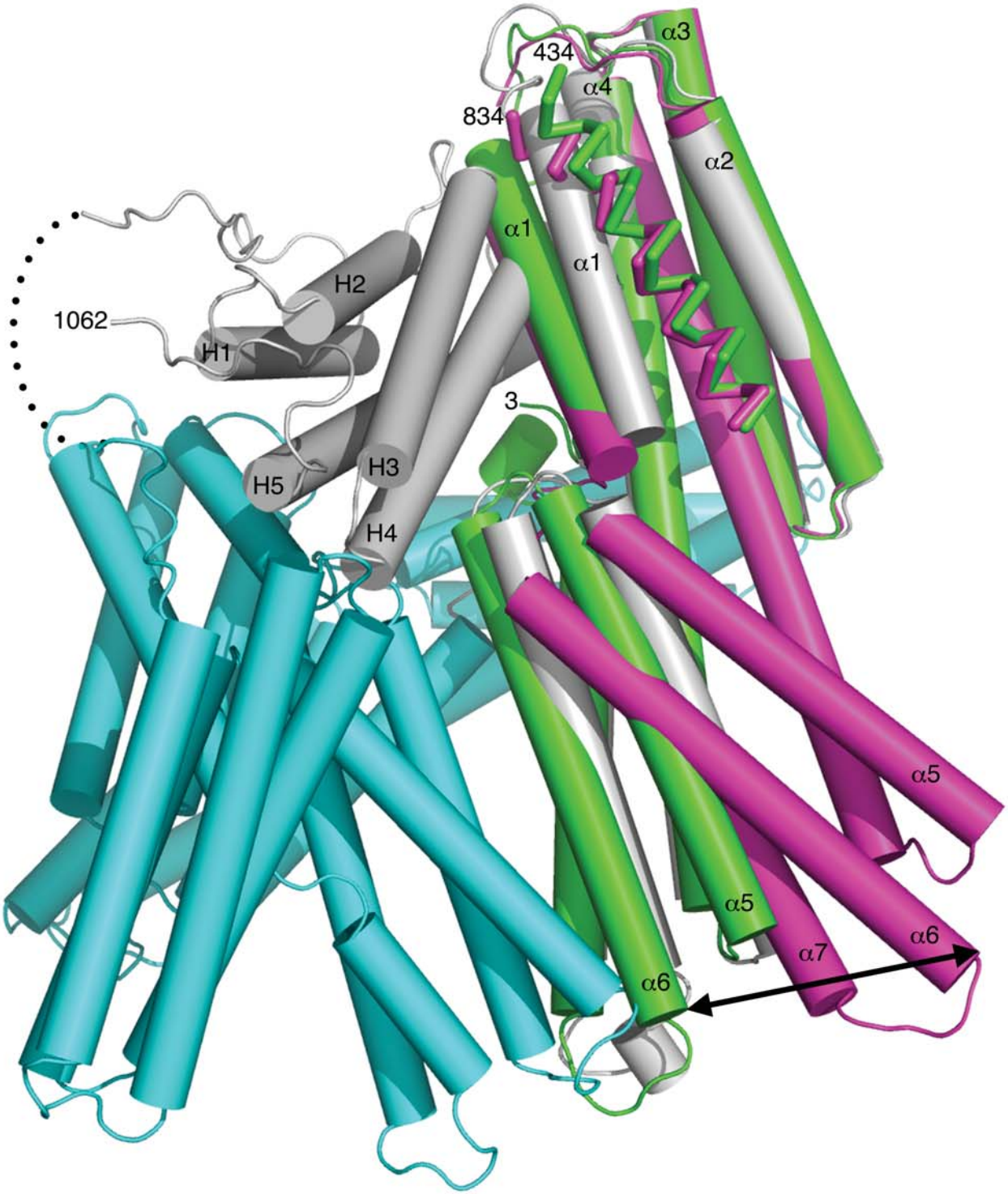

Supplementary Figure S9